

# PCCP

Accepted Manuscript



This is an *Accepted Manuscript*, which has been through the Royal Society of Chemistry peer review process and has been accepted for publication.

*Accepted Manuscripts* are published online shortly after acceptance, before technical editing, formatting and proof reading. Using this free service, authors can make their results available to the community, in citable form, before we publish the edited article. We will replace this *Accepted Manuscript* with the edited and formatted *Advance Article* as soon as it is available.

You can find more information about *Accepted Manuscripts* in the [Information for Authors](#).

Please note that technical editing may introduce minor changes to the text and/or graphics, which may alter content. The journal's standard [Terms & Conditions](#) and the [Ethical guidelines](#) still apply. In no event shall the Royal Society of Chemistry be held responsible for any errors or omissions in this *Accepted Manuscript* or any consequences arising from the use of any information it contains.

## Gold as *intruder* in ZnO nanowires

José M. Méndez-Reyes<sup>1</sup>, B. Marel Monroy<sup>1</sup>, Monserrat Bizarro<sup>1</sup>, Frank Güell<sup>2</sup>, Ana Martínez<sup>1</sup>, Estrella Ramos<sup>1</sup>

<sup>1</sup> Instituto de Investigaciones en Materiales, Universidad Nacional Autónoma de México. Circuito Interior, S N. Ciudad Universitaria. P.O. Box 70-360, Coyoacán, 04510. México DF, México

<sup>2</sup> Departament d'Electrònica, Universitat de Barcelona, C/Martí i Franquès 1, E-08028 Barcelona, Catalunya, Spain

### ABSTRACT

Several techniques for obtaining ZnO nanowires (ZnO NWs) have been reported in the literature. In particular, the vapour-liquid-solid (VLS) with Au as catalyst is widely used. During this process, Au impurities in the ZnO NWs can be incorporated accidentally, and for this reason we named these impurities as *intruders*. It is thought that these intruders may produce interesting alterations in the electronic characteristics of nanowires. In the experiment, it is not easy to detect either Au atoms in these nanowires, or the modification that intruders produce in different electrical, optical and other properties. For this reason, in this Density Functional Theory investigation, the effect of Au *intruders* in ZnO NWs is analysed. Au extended (thread) and point defects (atoms replacing Zn or O, or Au interstitials) are used to simulate the presence of gold atoms. Optimised geometries, band-gap and density of states indicate that the presence of small amounts of Au drastically modifies the electronic states of ZnO NWs. The results reported here clearly indicate that small amounts of Au have strong impact on the electronic properties of ZnO NWs, introducing states in the band edges that may promote transitions in the visible spectral region. The presence of Au as *intruders* in ZnO NWs enhances the potential use of this system for photonic and photovoltaic applications.

KEYWORDS: ZnO nanowires, density functional theory, electronic properties, density of states, Au intruders, photovoltaic applications

## Introduction

The new technological revolution is targeting the creation of nanodevices for optoelectronics, medicine, biology, sensor and energy applications, as they promise to be more efficient than the devices we already have. The specific characteristics of these nanodevices are attributed to the quantum confinement effect. One-dimensional nanostructures, such as nanowires (NWs) are used as building blocks for the construction of nanodevices. ZnO NWs are promising materials for several applications such as UV laser diodes,<sup>1, 2</sup> optical switches,<sup>3</sup> gas sensors,<sup>4, 5</sup> solar cells,<sup>6, 7</sup> photodetectors<sup>8</sup> and piezoelectric devices.<sup>9-11</sup> ZnO NWs are small crystalline materials with a large surface-to-volume ratio, which may prove useful for applications in future functional units for nanodevices.<sup>12</sup>

Several techniques for the growth of ZnO NWs have been reported in the literature. In particular, the vapour-liquid-solid (VLS) mechanism is widely used because it offers precise control of morphology for the growth of NWs, providing high-quality single-crystal materials, and it can be scaled up for industrial purposes.<sup>13</sup> The reactants are in vapour phase and supersaturate the liquid catalyst droplet. Employing a metal catalyst is mandatory for this technique and solid NWs are formed by precipitation from the droplet.<sup>14</sup> Au has been prolifically used as a catalyst because it produces more oriented NWs with fewer defects than other metals.<sup>12, 15-17</sup> An important factor is that Au used as catalyst can be accidentally incorporated during this process, producing impurities in the ZnO NWs. In this case, the presence of Au impurities in the ZnO NWs is not deliberate and for this reason we consider the Au atom as *intruder*. This is not a decorating process; nor is Au used as a dopant. In a decorating process, Au is employed to intentionally decorate ZnO NWs and Au nanoparticles remain at the surface of the nanowire,<sup>8, 12, 18-23</sup> modifying electrical, optical and other properties. There are scarce reports where ZnO NWs are intentionally doped with Au. In these systems, gold atoms are in the bulk, and some of the results indicate that Au-doping on ZnO NWs enhance particular properties.<sup>24</sup> When small amounts of Au are inserted unintentionally (as intruder), the metal atoms are also incorporated in the bulk of the ZnO NWs and alterations in the optical and electrical properties are to be expected. In spite of all the

reports describing decorating and doping ZnO NWs, few results have been presented with Au atoms as intruder in the ZnO NWs.

The role of Au as intruder in the opto-electronic properties of ZnO NWs remains to be explored in detail. However, there are some experimental results that report the photoluminescence emission spectra of single ZnO NWs, obtained using the VLS technique.<sup>25</sup> The authors associated an emission shoulder at 590 nm (2.10 eV), with the Au intruder introduced during Au-assisted catalytic growth. This experimental observation of radiative transitions in the visible region for single ZnO NWs is hypothetically related to the presence of Au intruders, but the experimental verification of this hypothesis is rather complicated, as only a few techniques permit atomic-scale visualization of Au impurities in semiconductors,<sup>26, 27</sup> not to mention the fact that sample preparation is often critical. Due to the catalytic process (mandatory in VLS), the presence of Au as intruder in ZnO NWs seems inevitable and for this reason it is imperative to understand the impact of gold intruders on these one-dimensional nanostructures.

Theoretical studies of atomic impurities in nanostructures have yielded very valuable information about the varied properties related to these systems. In particular, there are several theoretical analyses for ZnO NWs within the framework of Density Functional Theory (DFT). DFT has often been used to calculate the formation energies of ZnO nanostructures, as well as electronic and optical properties in either pristine or doped systems.<sup>28-31</sup> In fact, many efforts have been made to obtain accurate theoretical descriptions of these ZnO-based one-dimensional nanostructures.<sup>30-35</sup> The effects of atomic impurities in ZnO nanotubes<sup>29, 30</sup> and nanowires,<sup>32</sup> as well as the interaction between ZnO nanoclusters with Ag nanoparticles<sup>36</sup> have all been explored. However, no theoretical studies have previously been reported concerning the effect of Au intruders in the bulk (rather than superficial nanoparticles), on the properties of ZnO NWs. For this reason, the main goal of this investigation is to analyse the effect of Au atoms as intruders on the properties of ZnO NWs. In the following, we present a theoretical study of the effects of Au as extended and point defects on ZnO NWs. Optimised geometries, band-gap values, density of states (DOS), partial density of states (pDOS) and

molecular orbitals are used to explain the unique properties of the ZnO NWs, with Au as intruders.

## Methodology

### *Computational Details*

All calculations were carried out using Dmol3.<sup>37,38</sup> Electronic calculations were undertaken by applying the minimal basis set using effective core pseudopotential to describe the inner electrons of Zn and Au. The electrons considered explicitly for the calculations were: 2 electrons 1s, 2 electrons 2s and 4 electrons 2p for O, 2 electrons 3s, 6 electrons 3p, 10 electrons 3d and 2 electrons 4s for Zn, and finally 2 electrons 5s, 6 electrons 5p, 10 electrons 5d and 1 electron 6s for Au. It is noteworthy to point out that different basis sets (double zeta and effective core potential model) have been tested in order to find the optimal basis set for describing electronic properties and energetic stability in ZnO nanowires. The conclusions with the minimal basis set are the same as with the other basis set. We applied an orbital cutoff of 3.4 Ha. The exchange-correlation interaction was calculated with the generalised gradient approximation using the functional parameterised by Perdew, Burke, and Ernzerhof (PBE).<sup>39</sup> The convergence threshold for the self-consistent field, energy, gradient, and displacement was set to  $10^{-4}$ ,  $2 \times 10^{-2}$  Ha·nm<sup>-1</sup> and  $5 \times 10^{-3}$  nm, respectively, while the smearing was set to 0.02 Ha, for all calculations. The ZnO NWs were modelled using a supercell scheme described elsewhere<sup>40</sup>, from a bulk ZnO with hexagonal wurtzite structure. The supercell presents 432 atoms ( $a=b=32.49$  Å and  $c=20.82$  Å;  $\alpha=\beta=60^\circ$  and  $\gamma=90^\circ$ ). Each wire was placed in a supercell that has at least 10 Å between periodic replicas. This avoids spurious interactions between atoms belonging to vicinal cells due to the periodic boundary conditions imposed during the calculations.

To analyse the effect of the presence of Au on the electronic properties of nanowires, Zn<sub>54</sub>O<sub>54</sub> unit cell was used as a model. The diameter is 17.6 Å, measured from the farthest ends of the wire and the geometry was fully optimised. The band-gap values predicted by this model are very similar to those estimated for other ZnO nanostructures.<sup>21-28</sup> A bigger unit cell (Zn<sub>126</sub>O<sub>126</sub>, diameter equal to 22.7 Å) was also

calculated in order to analyse the band-gap values and the confinement effect. The band-gap of  $\text{Zn}_{54}\text{O}_{54}$  is similar to the band-gap of  $\text{Zn}_{126}\text{O}_{126}$ . Therefore, it is possible to say that  $\text{Zn}_{54}\text{O}_{54}$  is a good model for analysing systems with Au. The model used in this work predicts a bulk gap of 1.1 eV. This result concurs with other theoretical reports for bulk ZnO.<sup>41, 42</sup> It is well known that DFT underestimates the band-gap due to the reduction of correlation energy in *d* electrons, leading to an overestimation of the valence band energy.<sup>21,28,33,35</sup> However, it is important to note that in order to understand the effect of Au atoms in ZnO NWs, what matters is the change caused by the intruder. Since ZnO is a wide band gap material, experimentally it is expected that impurity levels will be located within the band gap.

#### *Incorporation of Au as an extended or a point defect*

The effect of Au was studied, contemplating the metal in three different positions: centre, middle and surface, using the  $\text{Zn}_{54}\text{O}_{54}$  unit cell. Au was located in the interstitial sites of the hexagon or substituting atoms, for each non-equivalent position. Two different defects were introduced: an extended defect, where interstitial Au atoms interacted with their periodic replicas (Au thread) and point defects, where “isolated” Au atoms substituted other atoms or acted as interstitial defects. For the study of Au as a thread, a short unit cell was chosen, while for the point defects, it is necessary to select a unit cell with more atoms in the NWs growth direction ([0001] in this case) to avoid spurious interaction between Au atoms in neighbouring cells. Importantly, after the incorporation of Au atoms in the system, all structures were optimised to the first and second nearest neighbours of the impurity. Figure 1 presents a scheme for the models with the notation used to distinguish between different positions. Partial densities of states (pDOS) were obtained considering the contribution of specific atom(s) onto the total density of states.

#### **Figure 1**

### **Results and Discussion**

#### *Geometry optimisation and stability*

Au atoms were placed in three non-equivalent positions in ZnO NWs (Figure 1). We estimated the relative energetic stability of the systems with Au, as a function of the formation energy according to the expression:<sup>40</sup>

$$E_f = E_{NW} - \sum_{i=Zn,O,Au} n_i \mu_i$$

Where  $E_{NW}$  is the ground-state energy of the nanowire,  $n_i$  indicates the number of the atomic species per supercell and  $\mu_i$  is the chemical potential of the more thermodynamically stable form, in each case (Zn hcp, Au fcc and O<sub>2</sub>), calculated using the same model.<sup>29, 43</sup> The calculation of the formation energy in semiconductors has been well established by Zhang and Northrup previously.<sup>44,45</sup> Due to the absence of experimental thermochemical data required in the model of Zhang and Northrup, other models are used recently for<sup>29,40</sup>. In this work we used the chemical potential for the reagents (Zn, O, Au in the most stable state) calculated with the same model used in the NWs as a reference in the formation of NWs.

Figure 2 reports the formation energy divided by the total number of atoms in each nanowire. The energy of the pristine ZnO NW (Zn<sub>54</sub>O<sub>54</sub>) is selected for reference. Negative values indicate more stable systems than the pristine nanowire.

## Figure 2

In Table 1, representative bond angles are included in order to analyse the distortion of the structures (the smaller the angle the greater the distortion). In all cases, structures with Au at the surface (Au<sub>s</sub><sup>k</sup>, O<sub>s</sub> or Zn<sub>s</sub>) are more distorted than structures with Au located at the centre or in the middle positions. The most distorted structures (less symmetric) are with an Au thread or interstitial located at the surface of the nanowires (Au<sub>s</sub><sup>th</sup> and Au<sub>s</sub><sup>i</sup>). This deformation stabilises the system ( $E_f$ /atom is -0.075 eV). Another parameter indicative of the distortion is how the diameter of the nanowire changes with the inclusion of the Au impurity. The diameter of the pristine ZnO NW is 18.123 Å. The diameters of the nanowires with impurities are reported in Table 1.

**Table 1.** Bond angles in degrees. Diameter of NW in (Å). The schematic representation of each angle is included in the Supplementary Information.

ZnO NW	Zn-Au-Zn (°)	Zn-O-Zn pristine NW (°)	O-Au-O (°)	O-Zn-O pristine NW (°)	Diameter NW (Å)
<b>Au<sub>c</sub><sup>th</sup></b>	90.0		95.2		18.068
<b>Au<sub>m</sub><sup>th</sup></b>	87.3		95.8		18.103
<b>Au<sub>s</sub><sup>th</sup></b>	79.2		66.0		18.123
<b>Zn<sub>c</sub></b>			118.7	114.5	18.192
<b>Zn<sub>m</sub></b>			103.3	113.0	18.161
<b>Zn<sub>s</sub></b>			93.1	107.4	16.866
<b>O<sub>c</sub></b>	110.9	116.4			16.246
<b>O<sub>n</sub></b>	110.9	118.2			16.246
<b>O<sub>s</sub></b>	78.7	122.9			17.512
<b>Au<sub>c</sub><sup>i</sup></b>	85.0		102.7		16.246
<b>Au<sub>m</sub><sup>i</sup></b>	96.2		79.8		16.246
<b>Au<sub>s</sub><sup>i</sup></b>	70.8		82.9		18.804

Concerning systems with Au in an interstitial position, ZnO NWs with Au at the surface of both models (extended (Au<sub>s</sub><sup>th</sup>) and point defect (Au<sub>s</sub><sup>i</sup>)) have negative values for  $E_f/\text{atom}$ . The others (Au<sub>c</sub><sup>th</sup>, Au<sub>m</sub><sup>th</sup>, Au<sub>c</sub><sup>i</sup> and Au<sub>m</sub><sup>i</sup>) are unstable with respect to the pristine ZnO NW (see Figure 2). This implies that Au may be preferentially located at the surface of the nanowire, when it is not incorporated into the ZnO NW lattice. In the case of Au replacing Zn (Zn<sub>c</sub>, Zn<sub>m</sub> and Zn<sub>s</sub>), the results are different from those with Au at the interstitial position. Stability is considerably diminished when the substitution occurs at the surface (Zn<sub>s</sub>), in comparison with Au located at the middle (Zn<sub>m</sub>) or at the centre (Zn<sub>c</sub>). Contrarily, when Au replaces O (O<sub>c</sub>, O<sub>m</sub> and O<sub>s</sub>), the structures are less stable

than ZnO NWs, in all cases. Thus, the system with Au replacing Zn is more stable than the system with Au replacing O.

### *Electronic properties*

The band-gap value obtained for the pristine ZnO NW is 1.23 eV. Figure 3 reports the band-gap for all systems being studied with Au in non-equivalent positions. Figure 3a shows that the presence of Au threads in the center and in the middle positions are equivalent, while for the surface position the band-gap diminishes slightly. For Au interstitials (Figure 3b), the band-gap is smaller with Au at the centre ( $Au_c^i$ ) or in the middle positions ( $Au_m^i$ ) than the corresponding value for  $Au_s^i$ . When Au substitutes Zn or O ( $Zn_j$ ,  $O_j$ ), the band-gap decreases from the center to the surface. The band-gap values of  $Zn_j$  (Figure 3c) defects are distinctly lower than the values for  $O_j$  defects (Figure 3d). From the experimental point of view, the decrease of the band-gap due to the presence of  $Zn_j$  defects in ZnO NWs implies that transitions between the band edges would be appreciably red-shifted in these systems. This might explain the experimental observation of radiative transitions in the visible region for single ZnO NWs, obtained using the VLS technique. Notably, the structural distortion induced by Au in the ZnO NWs is not always directly related to the decrease in the band-gap. For example, the most distorted structures present Au at the surface in all cases, but the band-gap trends for  $Au_s^i$  and  $Au_s^{th}$  are opposite. Therefore, the radiative transitions observed experimentally are not fully explained by geometric distortions.

### **Figure 3**

To gain insight into the nature of the electronic effects of Au intruders in ZnO NWs, Figure 4 reports the DOS focusing on the edges of valence and conduction bands for all systems being studied, including ZnO NW for comparison. The DOS representation shown in Figure 4 is useful for better understanding the electron density differences when Au is present and the relative energy shifts of states due to Au. In Figure 4a, it is possible to observe that in the case of  $Au_j^{th}$  the conduction band (CB) edge has shifted

to lower energy values, while the valence band (VB) is slightly shifted to higher energies. Similarly, in Figure 4b the presence of Au interstitials ( $\text{Au}_j^i$ ) produces a small displacement of the CB states to lower energy. However, the valence band (VB) only shifts to lower energy values for the superficial defect  $\text{Au}_s^i$ . This explains why the band-gap in the  $\text{Au}_s^i$  system increases with respect to  $\text{Au}_c^i$  and  $\text{Au}_m^i$ , *i.e.* there is a symmetrical energy displacement at the band edges. The shifts in CB induced by  $\text{Au}_c^i$  and  $\text{Au}_m^i$  explain the reduction of the band-gap in these cases. However, the most important shift in the CB edge occurs for the  $\text{Zn}_j$  replacements (Figure 4c indicated by the red arrow). This explains the marked decrease in the band-gap in cases where Au replaces Zn. Contrarily, in the case of  $\text{O}_j$  replacements (Figure 4d), the shift in the band edges is negligible and the band-gap remains almost the same for the systems, with or without Au atoms.

#### Figure 4

Another important observation related to the DOS is that for all the point defects where the occupied states (VB) exhibit a double peak, the energetic stability is less than for the ZnO NW (Figure 2). This is the case for all  $\text{O}_j$ ,  $\text{Zn}_s$ ,  $\text{Au}_c^i$  and  $\text{Au}_m^i$ . The systems with Au intruders, for which the shape of the VB DOS is similar to the ZnO NW (albeit displaced in energy), constitute the more stable systems, namely  $\text{Au}_s^{\text{th}}$ ,  $\text{Zn}_c$ ,  $\text{Zn}_m$  and  $\text{Au}_s^i$  (see Figure 2). It would appear that the electronic effect caused by the impurity is also related to the energetic stability of the system. In the case of the Au thread, the deformation of the VB in the case of the most stable structure ( $\text{Au}_s^{\text{th}}$ ) leads to a symmetric distribution of states. There may be two competing effects regarding the stability of the structures: the structural and the electronic deformations.  $\text{Au}_s^i$  and  $\text{Au}_s^{\text{th}}$  present important structural deformations, but the “deformation” of the electronic states due to the presence of Au is small in the former case and is symmetric in the latter case. This may indicate that the electronic effect counteracts the loss of structural symmetry, enabling the system to retain energetic stability.

HOMO and LUMO were obtained for all the systems being considered. All the molecular orbitals corresponding to the ZnO NW are p orbitals. No significant changes

are apparent when Au is introduced as a thread; whereas for the Au interstitials a very slight localisation around the Au impurity can be observed (these HOMO and LUMO are included as Supplementary Information). Figure 5 presents HOMO and LUMO for the systems with Au replacing Zn atoms. ZnO NW is included for comparison. Intense localisation of the HOMO around the Au impurity is evident in the case of Zn<sub>c</sub> and Zn<sub>m</sub>. These two systems are stable in terms of the  $E_f$  value reported in Figure 2. No significant changes are appreciated in the LUMO. The Au impurity has an effect on the electron density in all systems. Partial DOS (pDOS) corresponding to the Au atom and the replaced Zn atom are presented for each case. Notably, the Au atom introduces electronic levels at the edges of both the VB and the CB that Zn atoms do not exhibit.

### Figure 5

The HOMO and LUMO of the pristine ZnO NW indicate that HOMO is localised on the oxygen atoms and the LUMO is mainly localised at the oxygen atoms with a minor contribution of Zn atoms. Oxygen atoms would be prone to accept electrons derived from HOMO excitations. This implies that HOMO-LUMO transitions in the pristine NW would be favored mainly between oxygen atoms. In the Zn<sub>m</sub> case, HOMO and LUMO are located near to the Au intruder. Thus, HOMO-LUMO transitions would occur between the Au impurity and the anionic sublattice of the nanowire.

Trends concerning HOMO, LUMO and pDOS in the case of O<sub>j</sub> defects are shown in Figure 6. The only significant difference with respect to the ZnO NWs occurs when the Au atom is located at the surface. In this system, HOMO and LUMO are localised around the Au intruder. However, this localisation does not affect the band-gap significantly (Figures 3d and 4d). This may be due to the fact that both Au and O atoms have electronic states around the VB edge. In fact, the electronic states of the band edges in the pristine ZnO NW correspond mainly to O atoms. The O<sub>j</sub> substitutions have almost no effect on the distribution of electronic states at the band edges. Notably these systems are less stable than the pristine ZnO NW. Apparently, those systems with a large distortion in the electronic state distribution (Fig. 4b, c, d) are less stable than the pristine, as can be observed in Figure 2.

## Figure 6

A possible explanation of the effects of Au impurities on ZnO NWs is as follows: In the pristine ZnO NWs, the electronic levels at the band edges correspond mainly to the O atoms. Therefore, electronic transitions at the VB and CB edges occur preferentially between oxygen atoms, as indicated by the HOMO and LUMO of pristine ZnO NWs (see Figure 5), where the presented p orbitals are associated with O atoms with little participation of the Zn atom. When Au is introduced into ZnO NWs substituting Zn, the HOMO is localised around the Au atoms (Figure 5). This effect is due to the higher electronegativity of Au compared to the Zn atom (2.54 and 1.65, respectively). Au atoms derive electronic density from neighbouring Zn atoms, causing the observed shifts in the Zn electronic states. Furthermore, Au presents electronic levels at the VB edge, as shown in Figure 5 and therefore, electronic transitions would be likely to occur from the VB localised at the Au atoms to the CB localized at the O atoms. This may be the explanation for the experimental observation concerning radiative transitions in the visible region for single ZnO NWs with Au intruders. When Au replaces O, the effect is almost negligible and the systems are less stable than ZnO NW.

The above explanation will provide more insights concerning the experimental photoluminescence observation of single ZnO NWs. Our results indicate that the presence of Au impurities replacing Zn atoms modify the electronic states of the system. Because of the high localisation of the HOMO around Au impurities, it is likely that optical transitions would occur between Au and O. The observed decrease in the band-gap in these cases is consistent with the experimental observation of radiative transitions in the visible region for single ZnO NWs. From an experimental point of view, it is always desirable to have other measurable quantities to validate the theoretical calculations. In this case, the Ultraviolet Photoelectron Spectroscopy technique could be useful to obtain the electronic structure of the valence band in order to compare it with the calculated one. Besides the photoluminescence, the other physical property that may be affected by the presence of Au intruders is the electrical conductivity. Considering the semiconducting nature of ZnO, a small amount of impurities would be able to change not only the conductivity value, but also the nature of the charge carriers

(depending on the amount of Au); however, in practice very fine measurement methods are needed, such as Conductive Atomic Force Microscopy (C-AFM) that enables the correlation of the spatial feature of a ZnO NW with its conductivity or in the case of the photoluminescence the spectrally resolved Scanning Near-field Optical Microscopy, that has been successfully applied to detect the PL emission of a single ZnO NW<sup>13,25</sup>.

## Conclusions

Structural analyses of ZnO NWs with Au indicate that the metal atoms produce a geometrical distortion of the wires, but this deformation is not directly related to the electronic properties of ZnO NWs with Au. In the pristine ZnO NWs, the electronic levels at the band edges correspond mainly to the O atoms. Our results indicate that the presence of Au impurities replacing Zn atoms modify the electronic states of the system. Because of the high localisation of the HOMO around Au impurities, it is likely that optical transitions would occur between orbitals of Au and O. The observed decrease in the band-gap in these cases is consistent with the experimental observation of radiative transitions in the visible region, even for apparently single ZnO NWs. It is important to emphasise that our results indicate that even a small amount of Au (some Au atoms replacing Zn atoms) produces a strong effect on the electronic properties of the ZnO NWs. This result is relevant, as experimentally it is possible to observe radiative transitions in the visible region for single ZnO NWs, whereas it is not possible to easily detect Au atoms in ZnO NWs. The results reported here indicate that small amounts of Au produce strong effects in terms of the electronic properties of the NWs and therefore the electronic transitions between the band edges are significantly redshifted, enabling radiative transitions in the visible region. It can be concluded that Au is a convenient intruder in ZnO NWs as it increments the spectral range of band-to-band transitions from the UV to the visible, which may be very useful for future applications in photonics and photovoltaics, where this spectral range is of interest.

## Supplementary Information

Schematic representation of bond angles. HOMO and LUMO for Au interstitials: thread and point defects.

## **AUTHOR INFORMATION**

### **Corresponding Author**

\*Corresponding author's email:

### **Author Contributions**

The manuscript was written through contributions of all authors. All authors have given approval to the final version of the manuscript. The authors declare no competing financial interest.

### **Funding Sources**

This work was made possible due to the funding of DGAPA-PAPIIT through project IB101712, Consejo Nacional de Ciencia y Tecnología (CONACyT) through projects 153948 and 203519 and resources provided by the Instituto de Investigaciones en Materiales (IIM).

## **ACKNOWLEDGMENTS**

We would like to thank DGTIC of Universidad Nacional Autónoma de México (UNAM) for their excellent and free supercomputing services. We thank Caroline Karlake (Masters, Social Anthropology, Cambridge University, England) for reviewing the grammar and style of the text in English. The authors would like to acknowledge Oralia Jiménez, María Teresa Vázquez, Joaquín Morales, Alberto López and Caín González for their technical support.

## **ABBREVIATIONS**

ZnO NWs, zinc oxide nanowires; VLS, vapour-liquid-solid; DFT, Density Functional Theory; DOS, density of states; pDOS, partial density of states; CB, conduction band; VB, valence band; HOMO, highest occupied molecular orbital; LUMO, lowest unoccupied molecular orbital; PL, photoluminescence

## REFERENCES

1. S. Chu, G. Wang, W. Zhou, Y. Lin, L. Chernyak, J. Zhao, J. Kong, L. Li, J. Ren and J. Liu, *Nat Nano*, 2011, **6**, 506-510.
2. L. K. van Vugt, S. Rühle and D. Vanmaekelbergh, *Nano Letters*, 2006, **6**, 2707-2711.
3. L. X. Mu, W. S. Shi, T. P. Zhang, H. Y. Zhang, Y. Wang, G. W. She, Y. H. Gao, P. F. Wang, J. C. Chang and S. T. Lee, *Applied Physics Letters*, 2011, **98**, -.
4. N. Kumar, A. K. Srivastava, R. Nath, B. K. Gupta and G. D. Varma, *Dalton Transactions*, 2014, **43**, 5713-5720.
5. H. Minaee, S. H. Mousavi, H. Haratizadeh and P. W. de Oliveira, *Thin Solid Films*, 2013, **545**, 8-12.
6. C. Xu, J. Wu, U. V. Desai and D. Gao, *Nano Letters*, 2012, **12**, 2420-2424.
7. J. Fan, Y. Hao, C. Munuera, M. García-Hernández, F. Güell, E. M. J. Johansson, G. Boschloo, A. Hagfeldt and A. Cabot, *The Journal of Physical Chemistry C*, 2013, **117**, 16349-16356.
8. K. Liu, M. Sakurai, M. Liao and M. Aono, *The Journal of Physical Chemistry C*, 2010, **114**, 19835-19839.
9. S. Eustis, L. H. Robins and B. Nikoobakht, *The Journal of Physical Chemistry C*, 2009, **113**, 2277-2285.
10. B. J. M. Velazquez, S. Baskaran, A. V. Gaikwad, T.-T. Ngo-Duc, X. He, M. M. Oye, M. Meyyappan, T. K. Rout, J. Y. Fu and S. Banerjee, *ACS Applied Materials & Interfaces*, 2013, **5**, 10650-10657.
11. Y. Hu, B. D. B. Klein, Y. Su, S. Niu, Y. Liu and Z. L. Wang, *Nano Letters*, 2013, **13**, 5026-5032.
12. M. M. Brewster, X. Zhou, S. K. Lim and S. Gradečak, *The Journal of Physical Chemistry Letters*, 2011, **2**, 586-591.
13. F. Güell, J. O. Ossó, A. R. Goñi, A. Cornet and J. R. Morante, *Superlattices and Microstructures*, 2009, **45**, 271-276.
14. S. R. Hejazi, H. R. M. Hosseini and M. S. Ghamsari, *Journal of Alloys and Compounds*, 2008, **455**, 353-357.
15. K. A. Dick, *Progress in Crystal Growth and Characterization of Materials*, 2008, **54**, 138-173.
16. D. Ito, M. L. Jespersen and J. E. Hutchison, *ACS Nano*, 2008, **2**, 2001-2006.
17. Z. Zhu, T.-L. Chen, Y. Gu, J. Warren and R. M. Osgood, *Chemistry of Materials*, 2005, **17**, 4227-4234.
18. M. L. Sakurai, Kewei; Ceolato, Romain; Aono, Masakazu, *Key Engineering Materials*, 2013, **547**, 7-10.
19. T. X. Chen, G.Z.; Zhang, A.; Chen, H.Y.; Wu, T., *Nanotechnology*, 2008, **19**, 5.
20. M. d. L. P. Ruiz-Peralta, U.; Sánchez Zeferino, R., *ACS Applied Materials & Interfaces*, 2012, **4**, 4807-4816.
21. L. Z. Sun, Dongxu; Song, Zhiming; Shan, Chongxin; Zhang, Zhenzhong; Li, Binghui; Shen, Dezhen, *Journal of Colloid and Interface Science*, 2011, **363**, 175-181.
22. J. Z. Guo, Jun; Zhu, Min; Ju Dianxing; Xu Hongyan; Cao, Bingqiang, *Sensors and Actuators*, 2014, **199**, 339-345.

23. W.-Q. L. Zhang, Yang; Zhang, Tie-Kai; Xu, Weiping; Zhang, Meng; Yu, Shu-Hong, *J. Phys. Chem. C*, 2008, **112**, 19872-19877.
24. N. V. Hongsith, C.; Mangkorntong, P., *Ceramics International*, 2008, **34**, 823-826.
25. F. Güell, J. O. Ossó, A. R. Goñi, A. Cornet and J. R. Morante, *Nanotechnology*, 2009, **20**, 315701.
26. J. E. Allen, E. R. Hemesath, D. E. Perea, J. L. Lensch-Falk, LiZ.Y, F. Yin, M. H. Gass, P. Wang, A. L. Bleloch, R. E. Palmer and L. J. Lauhon, *Nature Nanotechnology*, 2008, **3**, 168-173.
27. A. A. Gunawan, K. A. Mkhoyan, A. W. Wills, M. G. Thomas and D. J. Norris, *Nano Letters*, 2011, **11**, 5553-5557.
28. S. Haffad, G. Cicero and M. Samah, *Energy Procedia*, 2011, **10**, 128-137.
29. G. Chai, C. Lin, J. Wang, M. Zhang, J. Wei and W. Cheng, *The Journal of Physical Chemistry C*, 2011, **115**, 2907-2913.
30. D. Q. Fang, A. L. Rosa, R. Q. Zhang and T. Frauenheim, *The Journal of Physical Chemistry C*, 2010, **114**, 5760-5766.
31. N. H. Moreira, G. Dolgonos, B. Aradi, A. L. da Rosa and T. Frauenheim, *Journal of Chemical Theory and Computation*, 2009, **5**, 605-614.
32. C. Wang, Y. Wang, G. Zhang, C. Peng and G. Yang, *Physical Chemistry Chemical Physics*, 2014, **16**, 3771-3776.
33. Z. Zhou, Y. Li, L. Liu, Y. Chen, S. B. Zhang and Z. Chen, *The Journal of Physical Chemistry C*, 2008, **112**, 13926-13931.
34. I. Khan and I. Ahmad, *International Journal of Quantum Chemistry*, 2013, **113**, 1285-1292.
35. S. Saha, S. Pal, P. Sarkar, A. L. Rosa and T. Frauenheim, *Journal of Computational Chemistry*, 2012, **33**, 1165-1178.
36. F. X. Sheng, Chunxiang; Jin, Zhulin; Guo, Jiyuan; Fang, Shengjiang; Shi, Zengliang; Wang, Jinlan, *The Journal of Physical Chemistry C*, 2013, **117**, 18627-18633.
37. B. Delley, *The Journal of Chemical Physics*, 1990, **92**, 508-517.
38. B. Delley, *The Journal of Chemical Physics*, 2000, **113**, 7756-7764.
39. J. P. Perdew, K. Burke and M. Ernzerhof, *Physical Review Letters*, 1996, **77**, 3865-3868.
40. A. C. Trejo, M.; Ramos, E.; Cruz-Irisson, M., *Nanoscale Research Letters*, 2012, **7**, 471.
41. B. F. Himmetoglu, Andrea; de Gironcoli, Stefano; Cococcioni, Matteo, *International Journal of Quantum Chemistry*, 2014, **114**, 14-49.
42. S. S. Saha, Sunandan; Pal, Sougata; Sarkar, Pranab, *The Journal of Physical Chemistry C*, 2013, **117**, 15890-15900.
43. V. G. C. Dobrovskii, G.E.; Sibirev, N.V.; Jabeen, F.; Harmand, J.C.; Werner, P., *Nano Letters*, 2011, **11**, 1247-1253.
44. S. B. Zhang and J. E. Northrup, *Physical Review Letters*, 1991, **67**, 2339-2342.
45. J. E. Northrup and S. B. Zhang, *Physical Review B*, 1993, **47**, 6791-6794.
46. R. Rurali and X. Cartoixà, *Nano Letters*, 2009, **9**, 975-979.

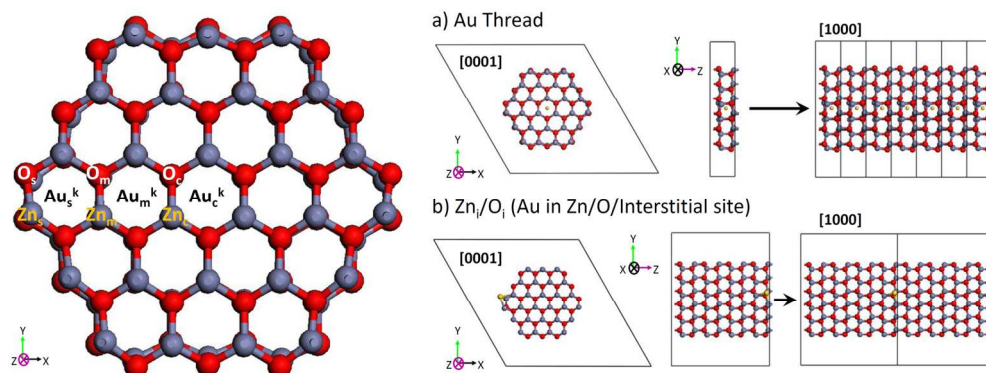


Figure 1. Left. Schematic representation of the Zn<sub>54</sub>O<sub>54</sub> model used for the study of Au effect in ZnO NWs.

The figure shows the non-equivalent positions where  $Au_j^k$ ,  $j=c$  (centre),  $m$  (middle) or  $s$  (surface), represents Au in an interstitial position as an extended defect (Au thread:  $Au_j^{th}$ ) or a point defect (Au interstitial:  $Au_j^i$ ) and  $O_i/Zn_i$ ,  $j=c$ ,  $m$  or  $s$ , represents the substitution of O or Zn by Au. Right. Schematic representation of the two different unit cells that were used for modelling a) Au as an extended defect (thread) and b) Au atoms as point defects. The different views correspond to the [0001] and [1000] directions as indicated in the figure.

160x64mm (300 x 300 DPI)

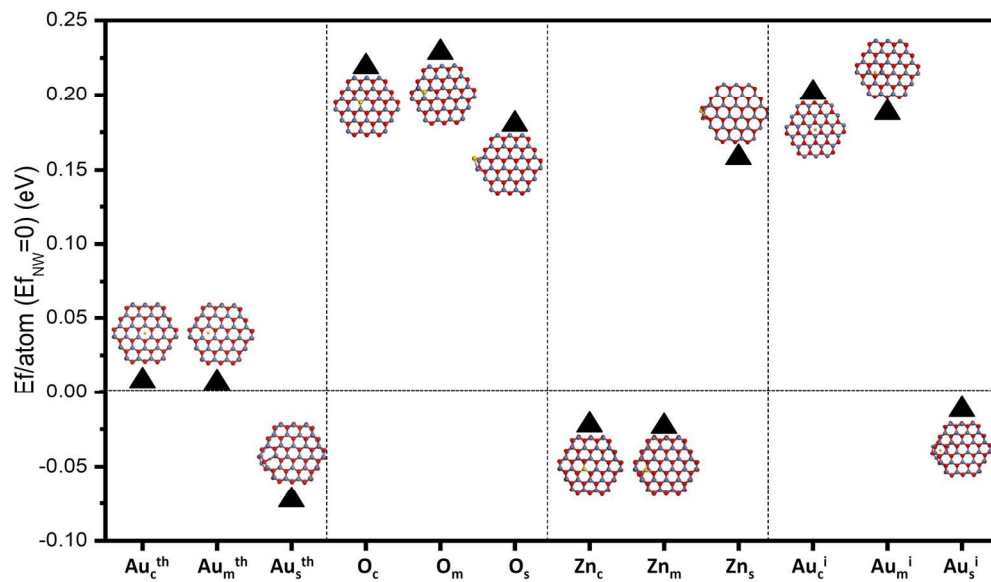


Figure 2. ZnO NWs structures with Au impurities in three different positions. The formation energy per atom ( $E_f/atom$ ) is compared between the structures, all referred to the ZnO NW without Au.  
160x94mm (300 x 300 DPI)

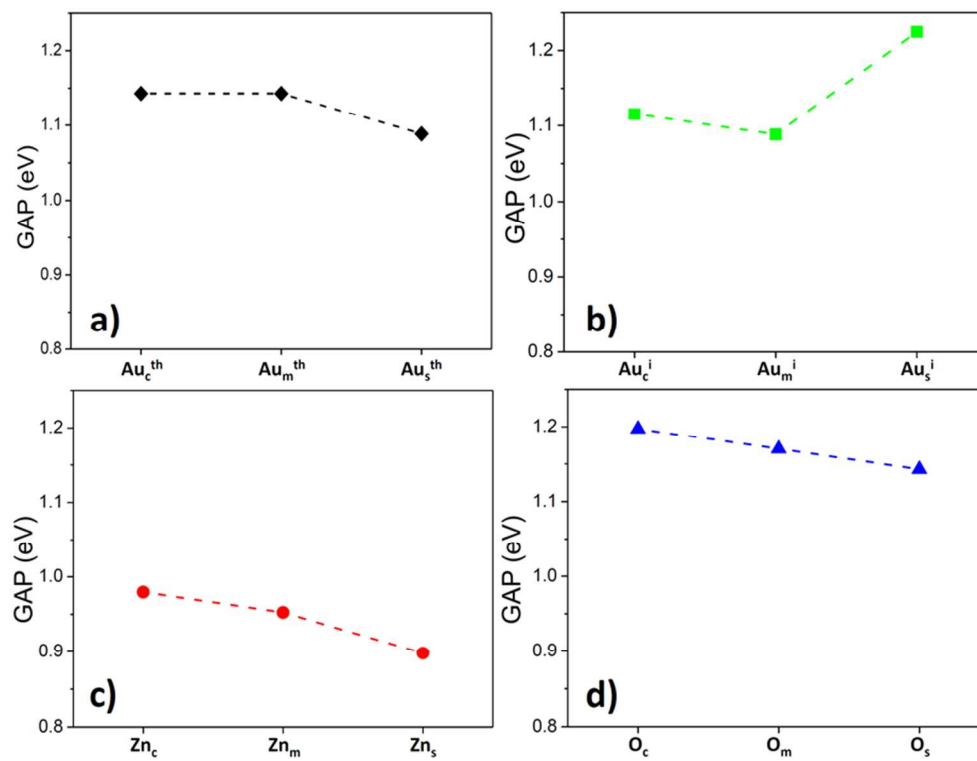


Figure 3. Band-gaps (in eV) of ZnO NWs with: a) Au thread, b) Au interstitial, c) Au in Zn site and d) Au in O site are reported. Lines are used as guide to the eye.  
80x60mm (300 x 300 DPI)

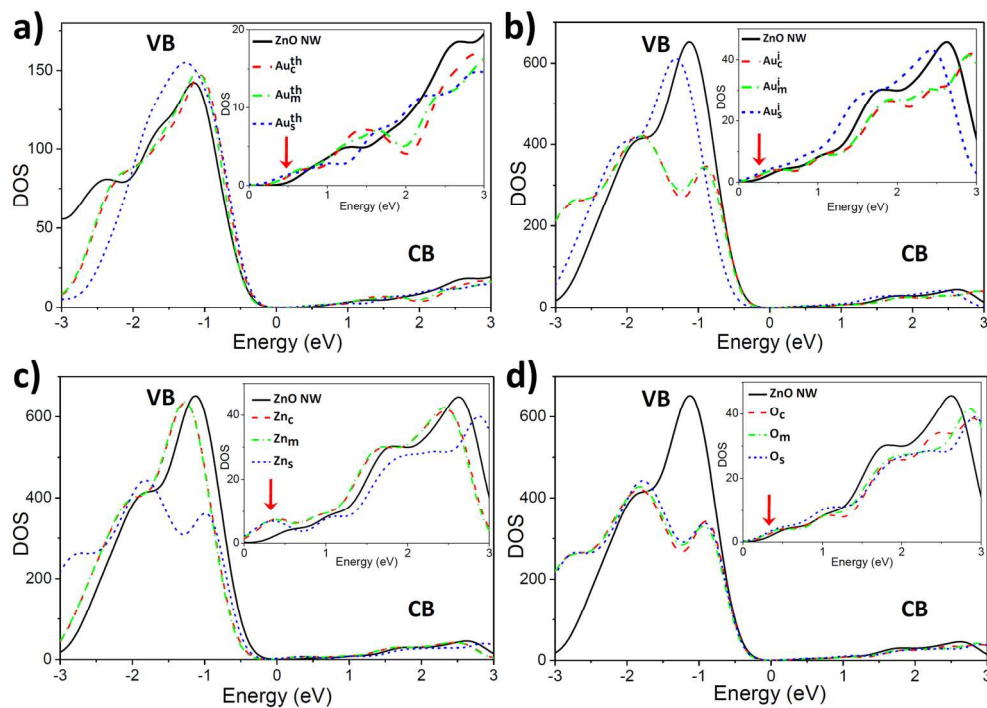


Figure 4. DOS (electrons/eV) focusing on the valence (VB) and conduction (CB) bands corresponding to ZnO NWs with a) Au thread, b) Au interstitial, c) Au in Zn site and d) Au in O site. The insets show the CB for better appreciation of the shifts indicated by red arrows. The selected smearing was 0.2 eV. The position of the Fermi level corresponds to zero in all cases.

160x113mm (300 x 300 DPI)

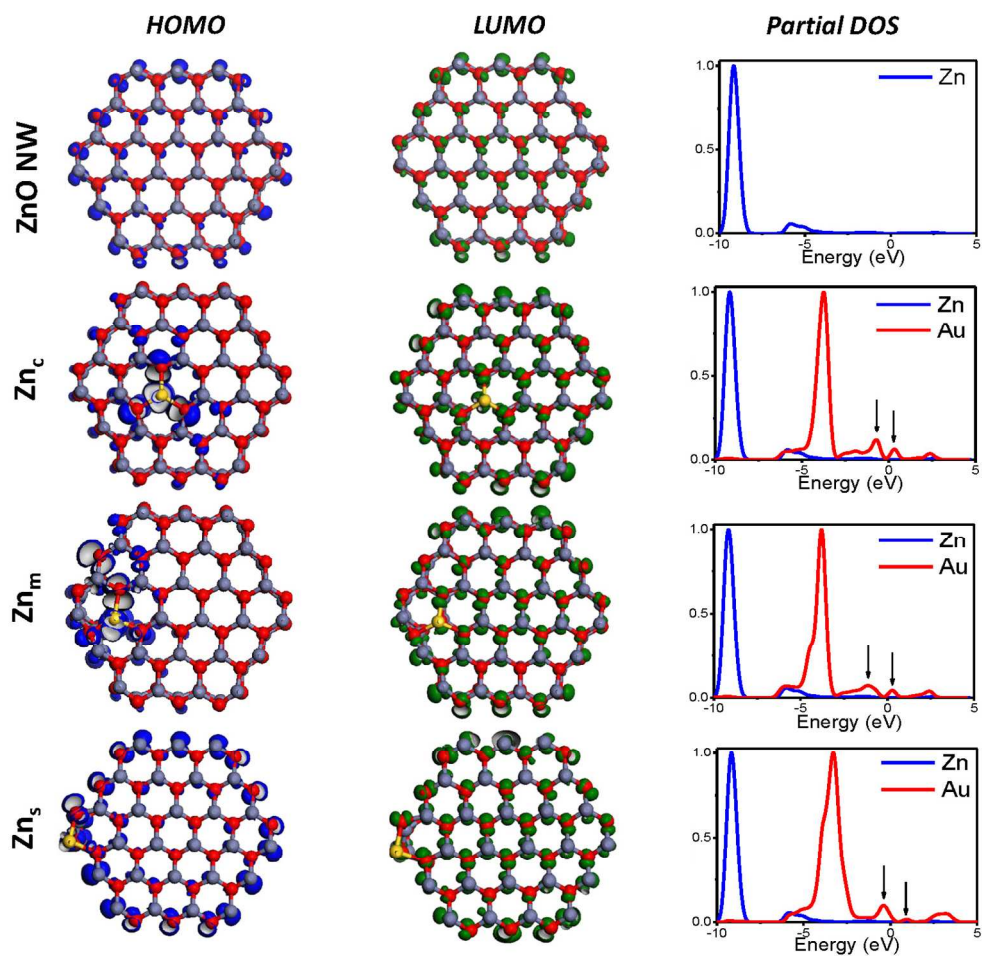


Figure 5. HOMO, LUMO and normalized pDOS of ZnO NWs with Au in Zn sites for the centre, middle and surface positions are presented. The arrows indicate the electronic states corresponding to Au at the VB and CB edges that Zn does not exhibit.  
303x290mm (139 x 139 DPI)

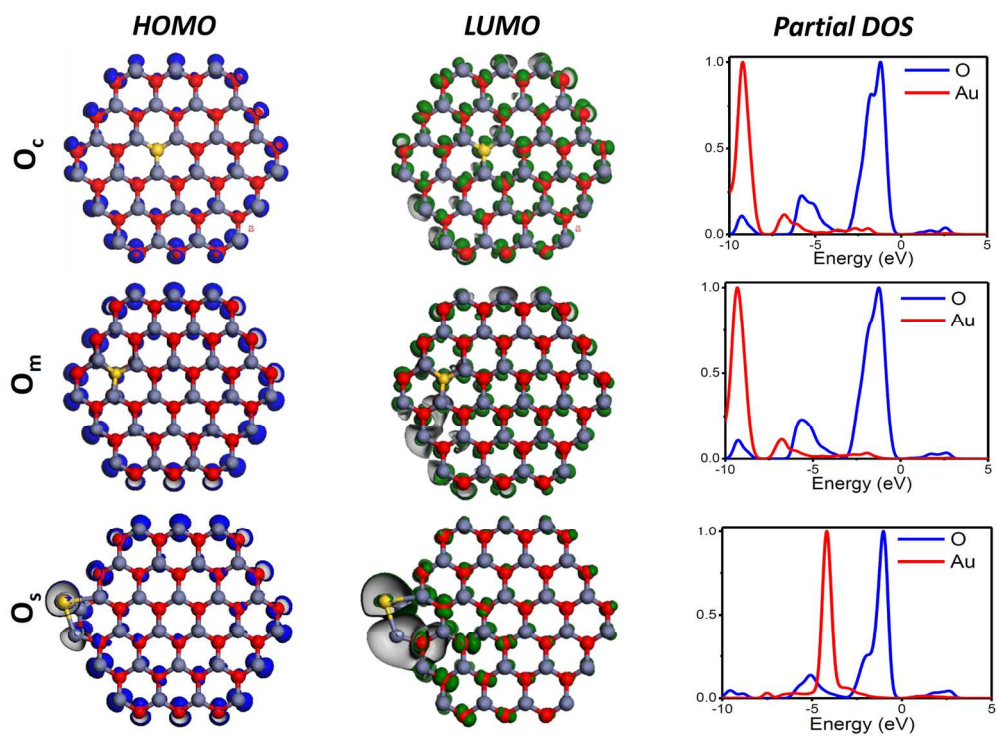


Figure 6. HOMO, LUMO and normalized pDOS of ZnO NWs with Au in O sites for the centre, middle and surface positions are shown.  
160x115mm (300 x 300 DPI)